NANO MICRO small

Supporting Information

for *Small,* DOI: 10.1002/smll.201700504

DNA-Assembled Core-Satellite Upconverting-Metal–Organic Framework Nanoparticle Superstructures for Efficient Photodynamic Therapy

Liangcan He, Michael Brasino, Chenchen Mao, Suehyun Cho, Wounjhang Park, Andrew P. Goodwin, and Jennifer N. Cha**

Submitted to ADVANCED MATERIALS

Supporting Information

DNA-Assembled Core-Satellite Upconverting-Metal Organic Framework Nanoparticle Superstructures for Efficient Photodynamic Therapy

Liangcan He, * *Michael Brasino, Chenchen Mao, Suehyun Cho, Wounjhang Park, Andrew P. Goodwin, Jennifer N. Cha* *

Dr. L. He, Dr. M. Brasino, Prof. A. P. Goodwin, Prof. J. N. Cha

Department of Chemical and Biological Engineering, University of Colorado, Boulder, CO, 80303 USA. E-mails: liangcan.he@colorado.edu; Jennifer.Cha@colorado.edu

C. Mao, S. Cho, Prof. W. Park

Department of Electrical, Computer and Energy Engineering, University of Colorado, Boulder, CO, 80303 USA.

Prof. W. Park, Prof. A. P. Goodwin, Prof. J. N. Cha

Materials Science and Engineering Program, University of Colorado, Boulder, CO, 80303 USA.

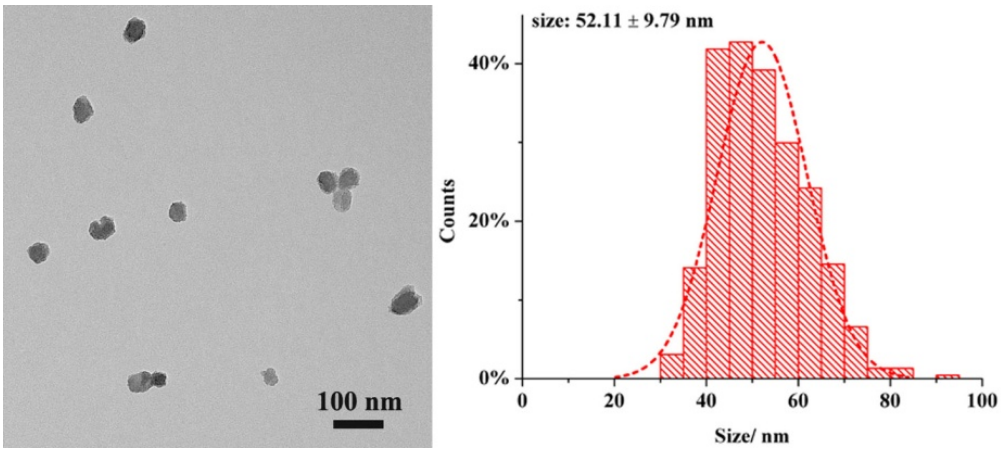

Figure S1. TEM images of PCN-224 MOF nanoparticles and particle size distribution which was determined by counting more than 300 particles.

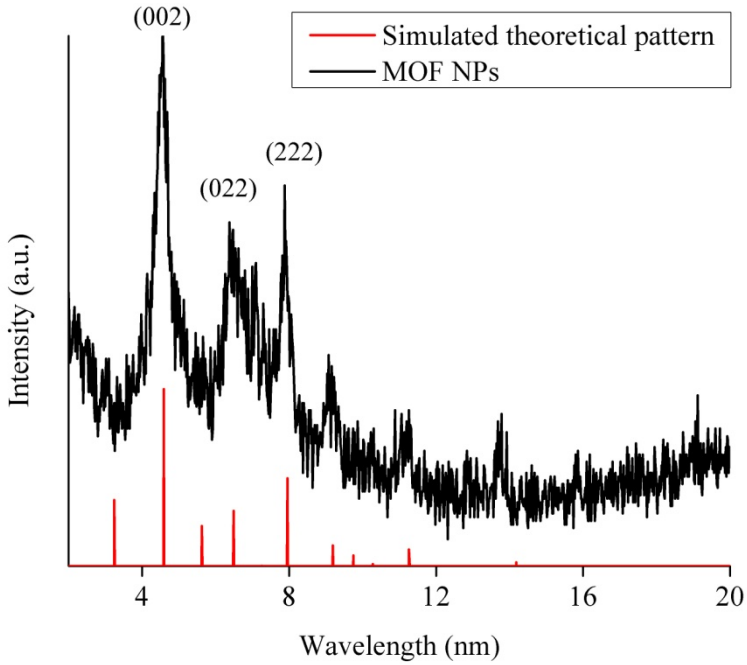

Figure S2. Powder XRD pattern of PCN-224 MOF NPs. The MOF NPs XRD pattern matches with the simulated theoretical one which indicates that the as-synthesized MOF NPs are crystalline and contain no other impurities.

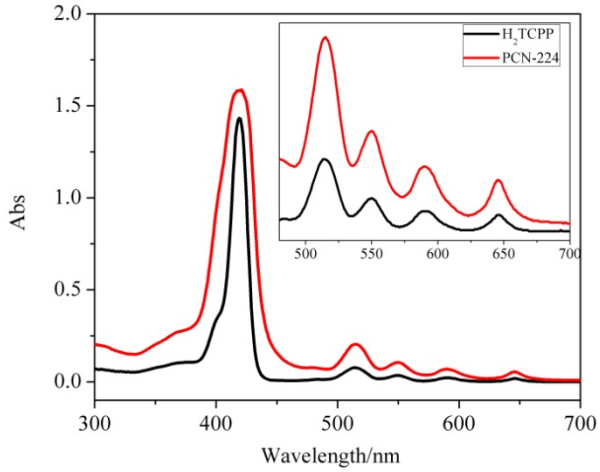

Figure S3. UV-Vis spectra of H_2TCPP and PCN-224 nanoparticles in DMF.

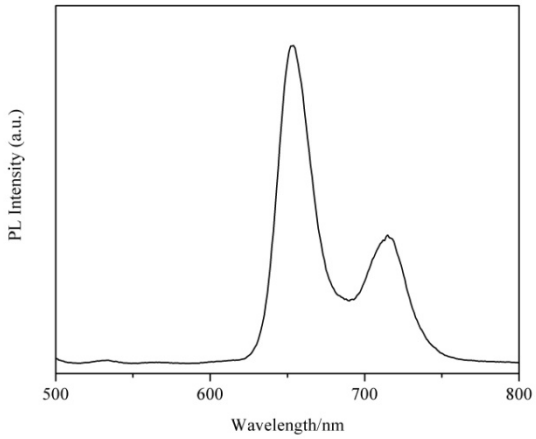

Figure S4. Emission spectra (λ_{ex} = 420 nm) of PCN-224 MOF NPs.

Table S1. DNA Sequences

DNA name	DNA usage	DNA sequence
DNA1	MOFs	5'-N_3-TTA TAA CTA TTC CTA AAA AAA AAA A-3'
DNA2	UCNPs	5'-N_3-TTT TTT TTT TTA GGA ATA GTT ATA A-3'

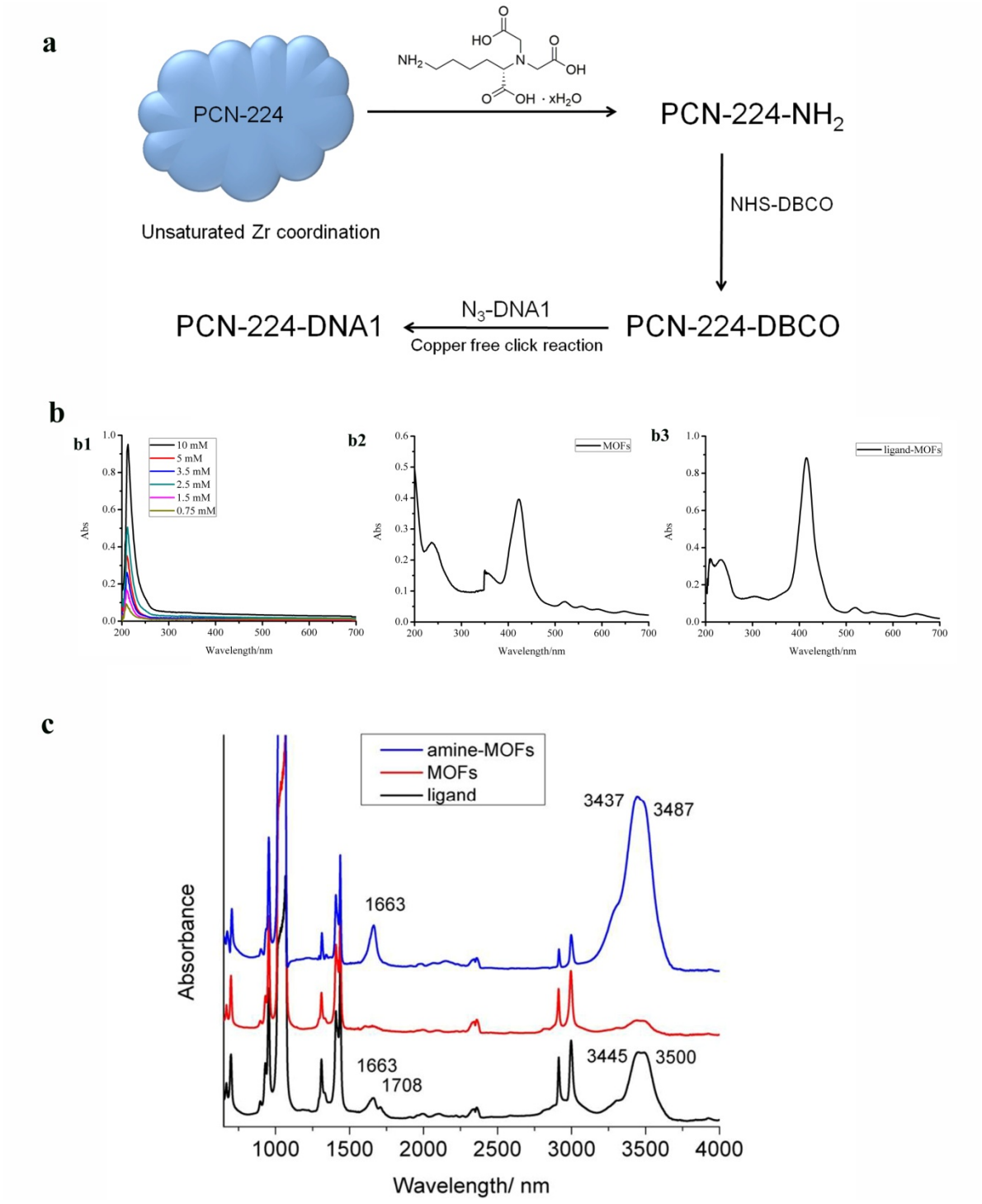

Figure S5. (a) Strategy used to modify PCN-224 MOF NPs with DNA strands.(b) UV-Vis spectra of the (b1) Nα,Nα-bis(carboxymethyl)-L-lysine hydrate (b2) MOFs and (b3) Nα,Nα-bis(carboxymethyl)-L-lysine hydrate conjugated MOFs. (c) FTIR sepctra of the ligand (Nα,Nα-bis(carboxymethyl)-L-lysine hydrate (black line), MOF NPs (red line) and amine-MOFs (blue line) DMSO solution.

The structure and composition of the Nα,Nα-bis(carboxymethyl)-L-lysine hydrate conjugated MOFs were investigated by Fourier transform infrared spectroscopy (FTIR) as shown in Figure S5c. Compared with the sepctrum of Nα,Nα-bis(carboxymethyl)-L-lysine hydrate, the asymemetric vibration band of carboxyl at 1708 cm^{-1} shifted to lower value around 1663 cm^{-1} in the FTIR spectrum of Nα,Nα-bis(carboxymethyl)-L-lysine hydrate conjugated MOFs,

indicating the formation of the coordination bonds between the carboxyl and metal ions in the MOF NPs. The two peaks around 3437 cm^{-1} and 3487 cm^{-1} could be ascribed to the asymmetric and symmetric stretching absorption of the primary amine groups. These spectra verify that the Nα,Nα-bis(carboxymethyl)-L-lysine hydrate was successfully conjugated to the MOF NPs. In addition, as is also shown in the UV-Vis spectra (Figure S5b), there is an obvious absorption peak at 213 nm which is indicative of the conjugated Nα,Nα-bis(carboxymethyl)-L-lysine hydrate.

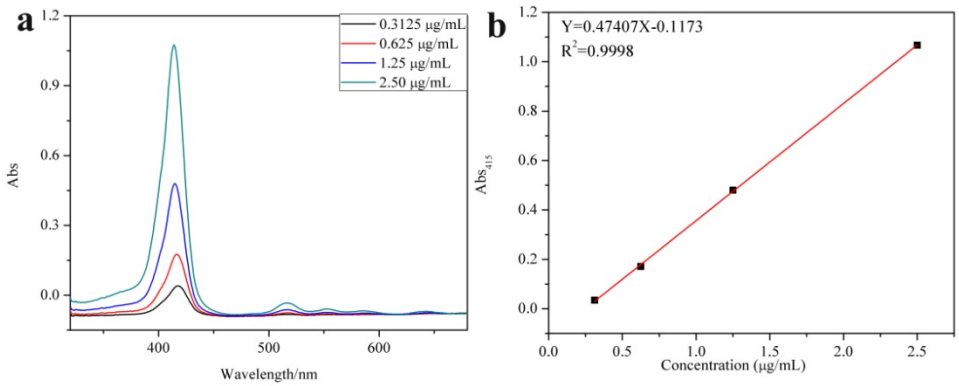

Figure S6. (a) UV-vis spectra of PCN-224 MOF NPs water solution at various concentrations; (b) calibration curve of PCN-224 MOF NPs at 415 nm.

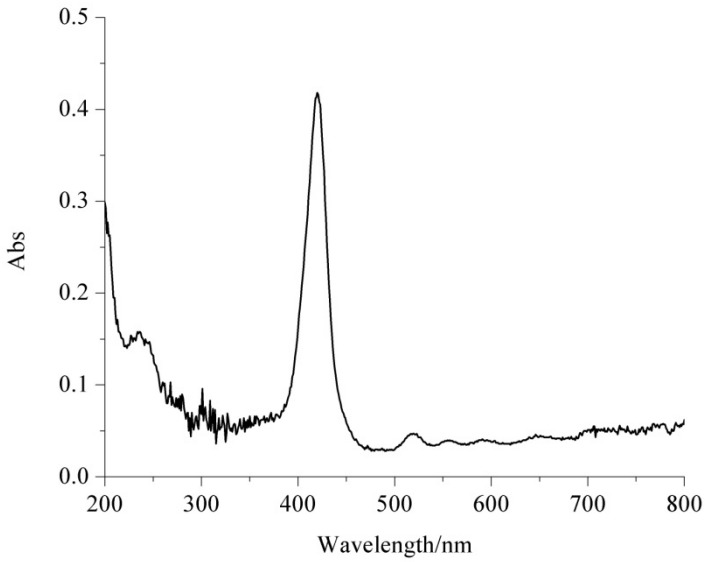

Figure S7. UV-vis spectra of DNA1-MOFs in aqueous solution. We estimated the amount of DNA bound per MOF NP by measuring the OD value at 260 nm of the supernatant after centrifuging out the MOF NPs. It should be noted that the calculation by UV-Vis is a rough estimation since there might be some nonspecific binding of DNA to the nanoparticle surfaces.

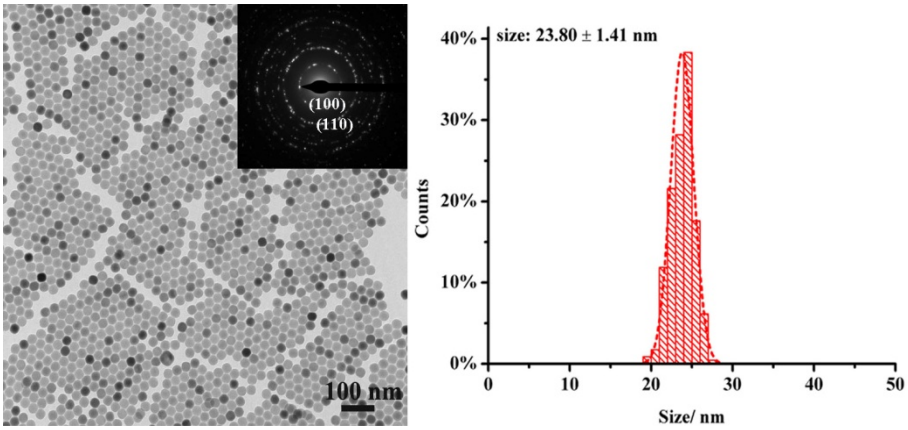

Figure S8. TEM images of $NaYF_4$,Yb,Er UCNPs and particle size distribution. Inset images in the TEM image is the selected area electron diffraction (SAED) pattern of the UCNPs. The SAED pattern shows crystalline diffraction rings corresponding to the (100), (110) planes of the β-phase $NaYF_4$lattice.

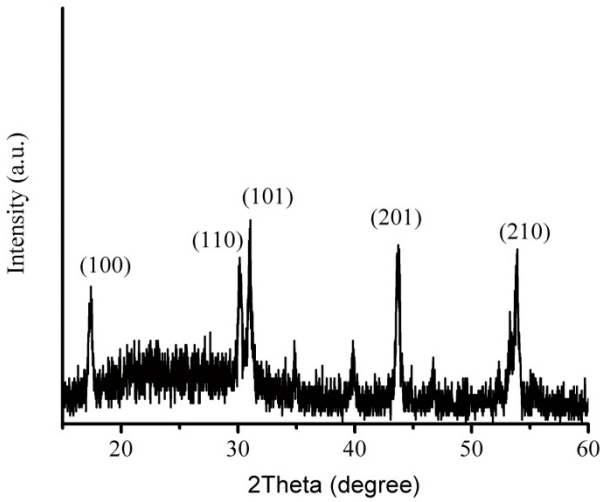

Figure S9. Powder XRD pattern of $NaYF_4$,Yb,Er UCNPs, the diffraction peaks also matching well with those calculated for the β-phase $NaYF_4$ (JCPDS PDF 28-1192).

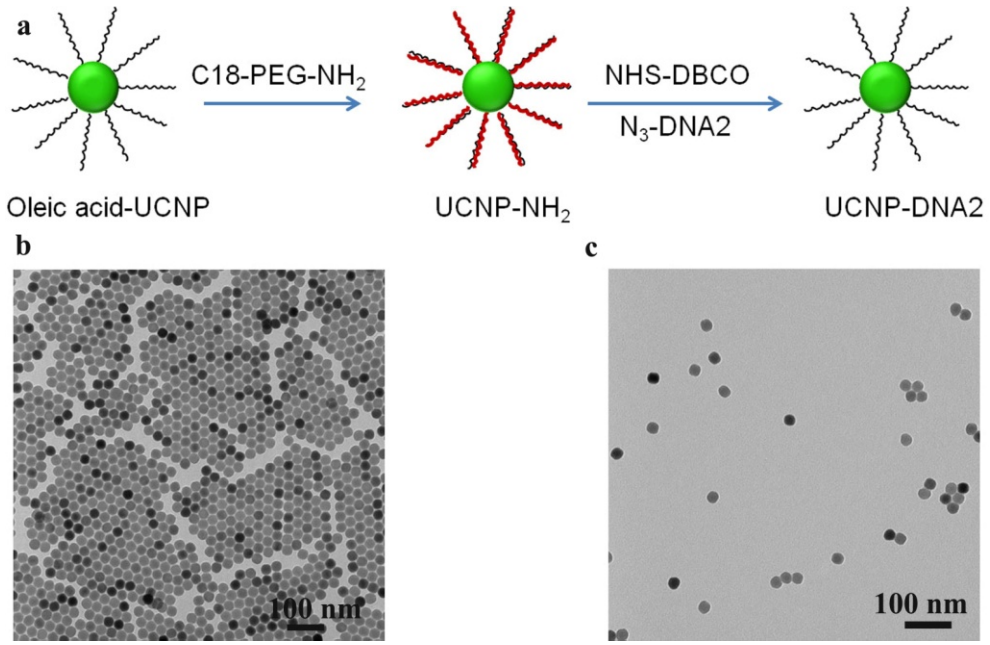

Figure S10. (a) Strategy for modifying UCNPs with DNA; (b) as-synthesized UCNPs; (c) the final DNA-UCNPs, which were well dispersed in water solution.

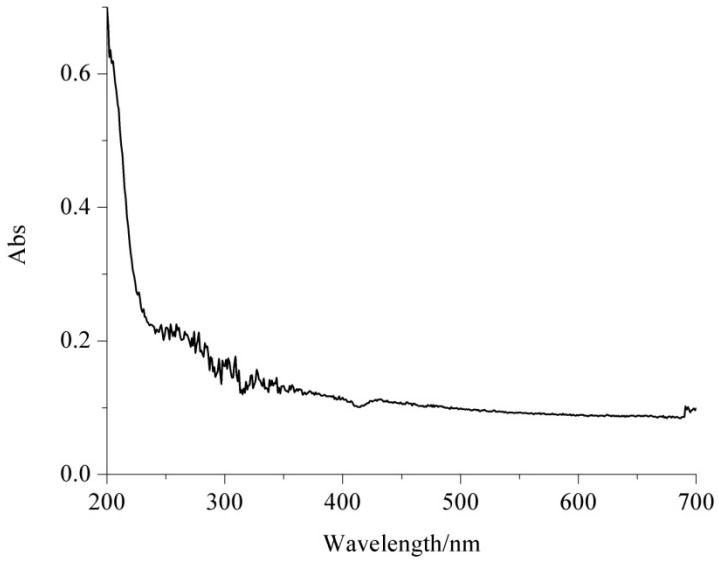

Figure S11. UV-vis spectra of DNA2-UCNPs in aqueous solution.

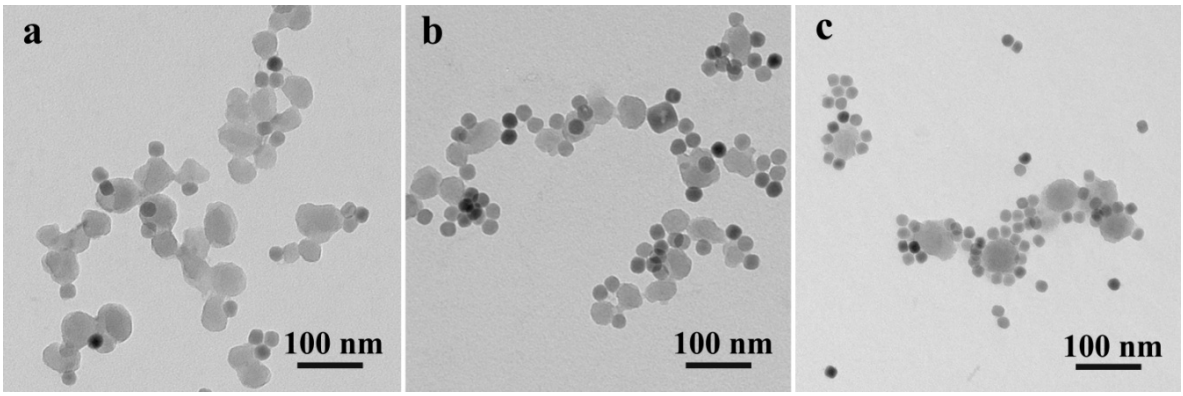

Figure S12. Low magnification TEM images of assembled MOF-UCNP structures using molar ratios of DNA1-MOF to DNA2-UCNP at: (a) 1:1; (b) 1:6; (c) 1:12.

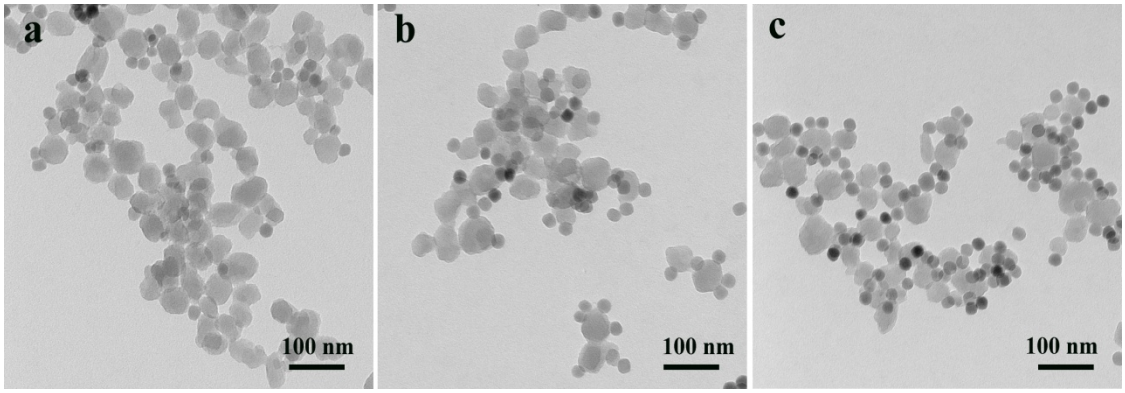

Figure S13. TEM images of assembled MOF-UCNP structures after 980 nm irradiation. The MOF-UCNP clusters shown were built using MOF:UCNP ratios of (a) 1:1; (b) 1:6; (c) 1:12.

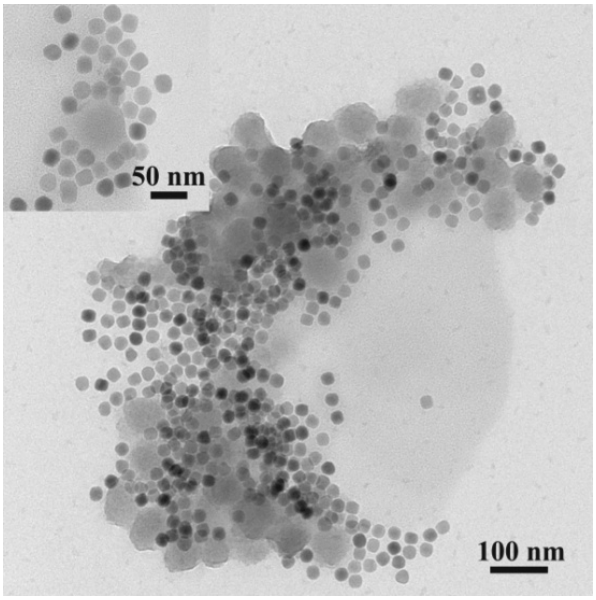

Figure S14. TEM images of DNA mediated MOF-UCNP assemblies using MOF:UCNP ratios of 1 to 24 (inset is the enlarged TEM imaging).

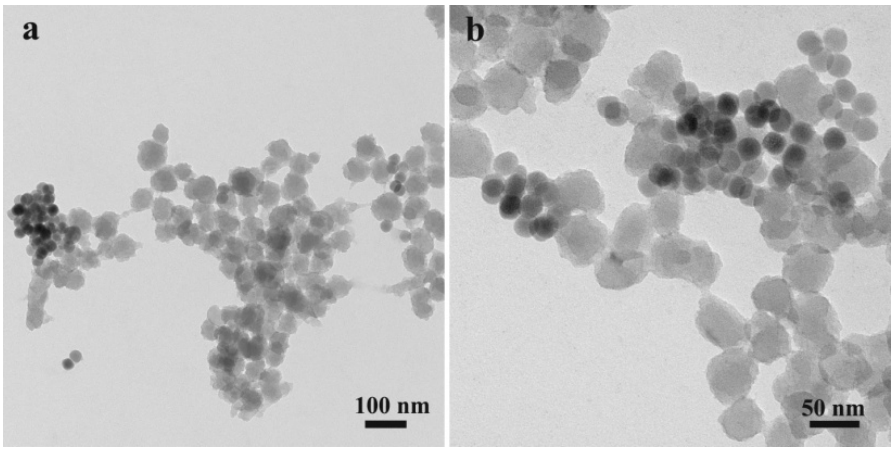

Figure S15. TEM images of DNA1-MOF NPs mixed with DNA1-UCNPs (noncomplementary DNA)

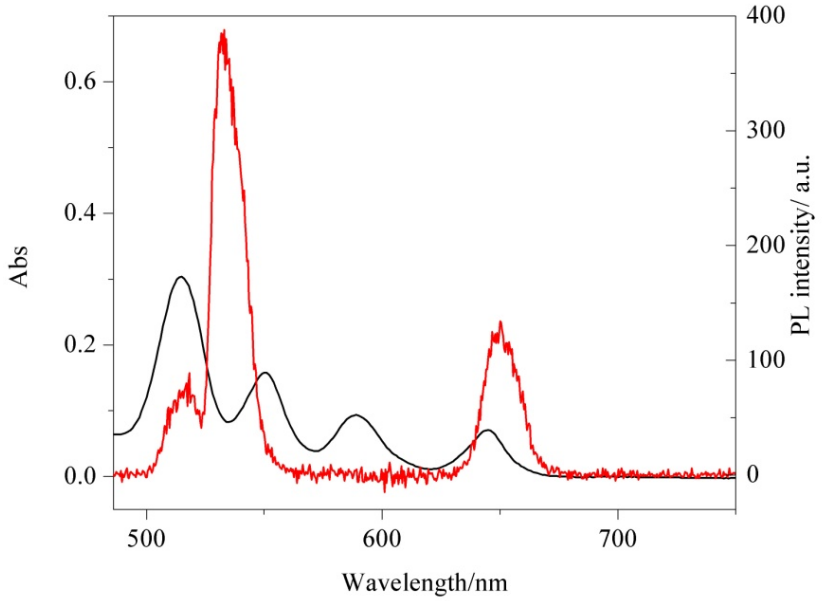

Figure S16. Photoluminescence spectra of the UCNPs under laser irradiation (λ_{ex} = 980 nm) (red line) and the absorption spectra of the PCN-224 MOF NPs (blank line).

Table S2. Quantitative analysis of the photoluminescence spectra of MOF-UCNP core-satellite structures and randomly mixed samples.

	MOF:UCNP=0:12	MOF:UCNP=1:12	MOF:UCNP (mix)=0:12
Green emission	100%	39.19%	57.00%
Absorbed green emission	--	60.81%	43.00%
Red emission	100%	65.09%	78.94%
Absorbed red emission	--	34.91%	21.06%

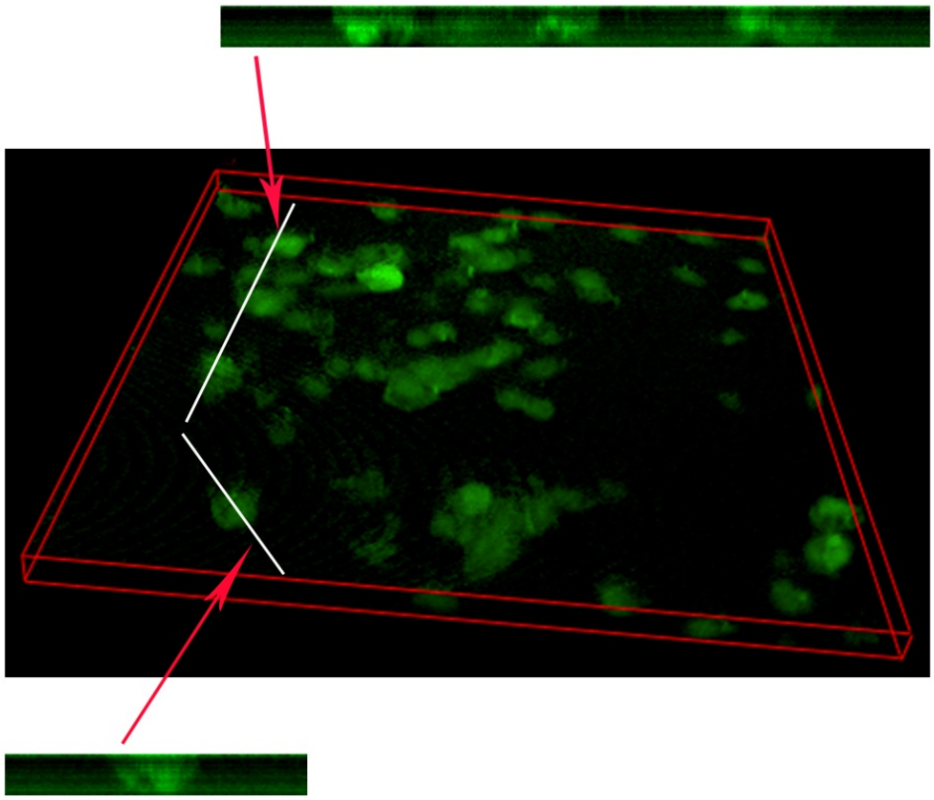

Figure S17. Cross section of the confocal image of of MDA-MB-468 cells incubated with MOF-UCNP$_{\text{affibody, fluorescence}}$ core-satellite superstructures.